SDC-91-00099
November 4, 1991

# Calorimetry Trigger Rates at the SDC

Greg Sullivan and Marshall Miller
*University of Chicago*

## 1 Introduction

In order to design a detector with a hardware trigger which will be efficient for interesting physics but will reduce backgrounds to a manageable level, we must answer certain critical questions. What is the trigger rate as a function of various sets of cuts? Given a specific set of cuts, what is the efficiency for tagging physics objects which constitute important physics signatures? In this note we present results using the ISAJET Monte Carlo to generate appropriate data sets and a fast detector simulation to model the detector and the trigger. We discuss rates relevant to Level 1 and Level 2 calorimetry triggers (i.e. jets, electrons, and photons).

Trigger decisions often require information from several detector components; for example, electrons triggers use the calorimeters, the tracking chambers, and the shower max detector. Our simulation must, therefore, include all these components. Detailed simulations of the tracking or calorimeters alone require large CPU times, and including both components would be prohibitive. Although we might like very accurate simulations, we don't need the level of detail present in many of the existing simulations. To answer the questions above we need a fast simulation so we can get first order results in reasonable times.

This note describes the simulation giving some details of the event generation and the detector model. Trigger rates and efficiencies are discussed, and the results of a study of electron backgrounds are presented.

# 2 Description of the Simulation

## 2.1 Event Generation

At the SSC design luminosity ($\mathcal{L} = 10^{33}$) the mean number of interactions per crossing is 1.6. We generated events by selecting a hard scattering event of interest (dijet, $W \rightarrow e\nu$, etc.) and overlayed N minimum bias events where N was taken from a poisson distribution with the mean equal to 1.6. Each event for a given interaction then had its vertex smeared along the beam direction using a gaussian distribution with the $\sigma = 3.4$cm.

All event samples were generated with the Isajet Monte Carlo. Minimum bias events were produced using the TWOJET event type and requiring $5 \leq p_T \leq 200$ GeV for each jet. Since calorimeter triggers are dominated by dijet production, we generated TWOJET event samples with $p_T$ ranges of 20 – 50 GeV (called TWOJET 20-50), 50 – 100 GeV (called TWOJET 50-100), and 100 – 200 GeV (called TWOJET 100-200) in order to get enough statistics. These samples were weighted by cross section and added when producing rate plots. Finally, we generated $W \rightarrow e\nu$ events to study electron efficiencies. All events were generated with the top mass equal to 150 geV.

## 2.2 Detector Simulation

The detector simulation inputs all particles for a given crossing and steps them through the detector volume using fast parameterizations to determine the tracking and calorimeter response. Presently, the muon detectors are not modeled in the program. Details of the simulation are given below.

All photons are checked to see if they converted in the tracking volume. The tracking volume has a radius of 1.7 m and extends to $|\eta| < 1.6$, and material equal to 20% of a radiation length at $\eta = 0$ is assumed to be spread uniformly throughout this volume. Photons can then convert with equal probability anywhere within R = 1.7m. Charged pions and kaons are also checked for decay-in-flight in the tracking volume. Presently bremsstrahlung is not included in the simulation.

All particles are propagated out to the face of the calorimeters. If a particle is charged, it is bent in a 2.0 tesla magnetic field while it is in the central tracking volume. Tracking information is used in the trigger only for central tracking (i.e. $|\eta| < 1.6$). The trigger $p_T$ resolution is given by:

$$\frac{\delta p_T}{p_T} = 3.0 * p_T.$$

The trigger efficiency is taken to be 100% (i.e. all real tracks are found, and no false tracks are found). The trigger $p_T$ is simply the "real" $p_T$ smeared by the resolution. The table below shows the relevant central tracking parameters used in the simulation.

| Central Tracking Parameter | Value |
|---|---|
| B Field (Tesla) | 2.0 |
| Tracking Radius (meters) | 1.7 |
| Coil Thickness (meters) | 0.11 |
| Radiation lengths at $\eta = 0$ | 0.2 |
| Coverage | $\mid \eta \mid < 1.6$ |
| Resolution ($\delta p_T/p_T^2$ $p_T$ in TeV) | 3.0 |

After the particles are stepped out to the calorimeter face, their energy is smeared with a gaussian resolution function, and shower parameterizations are used to deposit energy in a 9X9 array of calorimeter towers. The calorimeter resolutions and other parameters used in the simulation are shown in the table below. At present, the simulation does not include the forward calorimeters ($\mid \eta \mid > 3.0$).

| Calorimeter Parameter | Value |
|---|---|
| EM radiation lengths at $\eta = 0$ | 25.0 |
| Had interaction lengths central | 9.0 |
| Had interaction lengths endplug | 11.0 |
| Central $\eta$ coverage | 1.6 |
| Endplug $\eta$ coverage | 3.0 |
| EM resolution | $\delta E = .15\sqrt{E}$ |
| Had resolution | $\delta E = .40\sqrt{E}$ |
| EM resolution constant term | 0.01 |
| Had resolution constant term | 0.02 |

The shower parameterizations were determined from testbeam data and incorporate fluctuations in both longitudinal and transverse directions. The longitudinal electromagnetic calorimeter parameterization was taken from the CDF detector simulation [1]. We used parameterizations for the transverse electromagnetic response and both the longitudinal and the transverse hadronic responses given to us by Ed Wang [2].

The simulation code allows users to input an electronics front end shaping function for the calorimeter response. This function determines the calorimeter response for each 16 nsec period after the particle hits the calorimeter. For shaping times longer than 1 beam crossing (16 nsec), the calorimeter response at any given crossing will be affected by the energy flow in events preceeding the crossing of interest. In this case the simulation throws minimum bias events for the appropriate number of crossings prior to the crossing of interest and uses the shaping function to sum up the energy in each calorimeter tower. The results discussed here all use a shaping time of 1 crossing so this feature was essentially turned off.

After all the particles are showered in the calorimeter, an array of trigger tower energies is created. The array stores hadronic and electromagnetic energy separately. In the central region ($\mid \eta \mid < 1.6$) trigger towers are assumed to be $2 \times 2$ sums of detector towers (i.e. $0.1\eta \times 0.1\phi$) giving a total of $16\eta \times 64\phi$ towers in central. The

endcap region ($1.6 <| \eta |< 3.0$) has varying segmentation with a total of $8\eta \times 64\phi$ towers per end. We used the trigger tower arrays for all rate and efficiency studies.

# 3 Results

## 3.1 Trigger Rates

In this section we discuss trigger rate studies for jets, electrons, and W's. The rates for electrons are found using the TWOJET event samples (i.e. all events are background). For each study we define the variation in algorithms used and present plots of cross sections versus threshold energies. The cross sections are given in millibarns. Note that at $\mathcal{L} = 10^{33}$:

$$1\text{mb} \rightarrow 1\text{MHz}$$

$$10^{-3}\text{mb} \rightarrow 1\text{kHz}$$

The expected trigger rates are:

$$\text{Level1} : 10^3 - 10^5\text{Hz}$$

$$\text{Level2} : 10^2 - 10^4\text{Hz}$$

Of course, rates for individual triggers (i.e. jet, electron, muon, ...) will be some fraction of the overall rate.

The jet trigger algorithm we used sums all the energy (both EM and Had) in an $N \times N$ array of trigger towers where N = 2, 4, or 8. We used fixed arrays of towers rather than centering the array on a seed tower. Figure 1 shows the trigger rate for each array size as a function of $E_T$. The difference in rate between array sizes of $8 \times 8$ and $2 \times 2$ is roughly a factor of 7.

The electron trigger algorithms involve 4 cuts with varying thresholds. All rates are shown as a function of the $E_T$ in an electromagnetic trigger tower and are usually plotted for several combinations of cuts. The Had/EM cut is the ratio of hadronic to electromagnetic energy in the trigger tower. The isolation cut (Iso) sums the hadronic trigger tower energy in the 8 trigger towers bordering the trigger tower of interest and divides by the electromagnetic energy in the trigger tower of interest. We also cut on the $p_T$ of a track pointing at the electromagnetic trigger tower. We assume only central tracking will participate in the trigger. We further assume the trigger will not have access to tracking $\eta$ information (other than $\pm\eta$) so any track pointing to the same $\phi$ bin as the electromagnetic trigger tower (64 bins in $\phi$) is taken to be a track match. All tracks used in the trigger are required to have $p_T > 10$GeV.

Figure 2 shows the cross section for TWOJET events passing various electron algorithms in the central region. The 4 curves are for $E_T$ only, Had/EM $< 0.05$, Had/EM $< 0.05$ plus Iso $< 0.07$, and Had/EM $< 0.05$ plus Iso $< 0.07$ plus $p_T >$ 10GeV. The strictest cut give a central electron rate of roughly 2 kHz at 20 GeV. Figure 3 shows the same rates for the endplug region. Here there is no tracking cut. Figure 4 shows the combined cross section for central and endplug electron triggers.

The curve with the $p_T$ cut applies the track cut only in the central. Figure 5 shows the cross section for the strictest set of cuts (Had/EM $< 0.05$, Iso $< 0.07$, and a central $p_T$ cut) with different $E_T$ thresholds in the central and endplug regions.

Figure 6 shows the cross section for $W \rightarrow e\nu$ triggers as a function of $E_T$ for various cuts. The efficiency for triggering on isolated electrons is shown to be very close to 100% at $E_T > 20$GeV for these cuts. The rate for $W \rightarrow e\nu$ triggers at a threshold of 20 GeV for $\mathcal{L} = 10^{33}$ is about 6 Hz. Figure 7 shows the $W \rightarrow e\nu$ cross section for the strictest set of cuts and different thresholds for central and endplug. Figure 8 shows the TWOJET background cross section versus the $W \rightarrow e\nu$ cross section for various sets of cuts. The increase in accepted W cross section above $6 \times 10^{-4}$mb is negligible since nearly all the remaining cross section is outside the defined fiducial region ($| \eta |< 3.0$). Finally, figure 9 and figure 10 show isolation or Had/EM versus $E_T$ for TWOJET events and $W \rightarrow e\nu$ events.

## 3.2 Electron Background Study

The prompt electron rate at Level 1 and Level 2 is dominated by background. The background processes are overlap between a charged hadron and a photon or $\pi^0$, a charged hadron showering early in the electromagnetic calorimeter, or a photon conversion. Understanding the relative rates of these backgrounds can be very useful for designing electron triggers because emphasis can then be placed on the trigger information which best reduces dominant backgrounds. Simple shower max information can significantly reduce backgrounds from overlaps but cannot easily reduce conversions or early showering pions. Information from the silicon tracker (or reducing the tracking volume mass) can reduce the conversion rate.

To study electron backgrounds we created an array of trigger towers and stored the $E_T$, particle ID, $\eta$, and $\phi$, for the 4 largest $E_T$ particles incident on the trigger tower. For all electron candidates we could then use this information to determine the most likely background process. We then defined 5 "electron" categories:

- Overlap (O). The electron trigger tower contained a photon with $p_T > 5$GeV but did not contain a conversion or a real electron. The trigger track was not a conversion.

- Early Showering Pion (S). The electron trigger tower contained no photons, real electrons, or conversions with $p_T > 5$GeV. The trigger track was in the same tower.

- Conversion (C). There was a conversion with $p_T > 5$GeV in the electron candidate trigger tower.

- Overlap Conversion (OC). The trigger track was not in the same trigger tower as the electron candidate, and the trigger track was a conversion.

- Electron (E). Non of the above (i.e. there was a real electron in the electron candidate trigger tower).

We used 2 sets of electron cuts (Loose and Tight) shown below.

| | $E_T$ (GeV) | Had/EM | Isolation | $p_T$ (GeV) |
|---|---|---|---|---|
| Loose Cuts | 10 | 0.07 | 1.0 | 5 |
| Tight Cuts | 10 | 0.05 | 0.07 | 5 |

We looked at data from 2000 TWOJET 20-50 events, 800 TWOJET 50-100 events, and 500 TWOJET 100-200 events. The number of electron candidates from these data sets falling into the various categories is shown below for the 2 sets of cuts.

| Category | Loose Cuts | Tight Cuts |
|---|---|---|
| O | 17 | 8 |
| S | 15 | 5 |
| C | 30 | 27 |
| OC | 9 | 6 |
| E | 4 | 3 |

These events are further divided into electron candidates with $p_T < 30$GeV and with $p_T > 30$GeV below.

| Category | Loose Cuts $p_T < 30$GeV | Tight Cuts $p_T < 30$GeV |
|---|---|---|
| O | 11 | 6 |
| S | 13 | 4 |
| C | 18 | 18 |
| OC | 6 | 4 |
| E | 3 | 2 |

| Category | Loose Cuts $p_T > 30$GeV | Tight Cuts $p_T > 30$GeV |
|---|---|---|
| O | 6 | 2 |
| S | 2 | 1 |
| C | 12 | 9 |
| OC | 3 | 2 |
| E | 1 | 1 |

As expected, the tight cuts reduce the rate of overlap and early showering pions more than the rate of conversions (pions have a broader Had/EM response). The only major difference between electron candidates with $p_T < 30$GeV and those with $p_T > 30$GeV is that the Had/EM cut eliminates more high $p_T$ candidates in the early showering pion category. For loose cuts, conversions (C + OC) constitute roughly 50% of the background. For tight cuts conversions are roughly 2/3 of the background.

The numbers above are useful in comparing the relative rates from different types of backgrounds, but we need more work to compare these rates to the real prompt electron signal (especially from b quark production). If the prompt electron signal is significant compared to certain backgrounds, working hard to reduce these backgrounds in the hardware trigger would be unproductive.

Clearly conversions dominate the background. Unless the tracking volume material is reduced, Level 2 algorithms which recognize conversions (such as using the silicon tracker to signal the absence of hits in the inner layers) must be used to reduce the rates appreciably. There are several shower max detector trigger algorithms. First, one could simply match hits in the shower max with the extrapolated track position. This algorithm reduces overlaps, has a smaller effect on early showering pions, and has no effect on conversions. Second, one could reconstruct the shower profile and compare with the expected profile from electrons. This algorithm would be much more effective against showering pions and conversions. While the simpler algorithm could be used at Level 1 times, reconstructing shower profiles would require too much time for Level 1. Since conversions cannot be tagged in Level 1, shower max trigger information will probably not be useful at that time.

# References


[1] J. Freeman and A. Beretvas, *Proceedings of the 1986 Summer Study on the Physics of the Superconducting Supercollider*, p. 482-6, Snowmass, (1986).

[2] Ed Wang,*SSCL*, private communication.

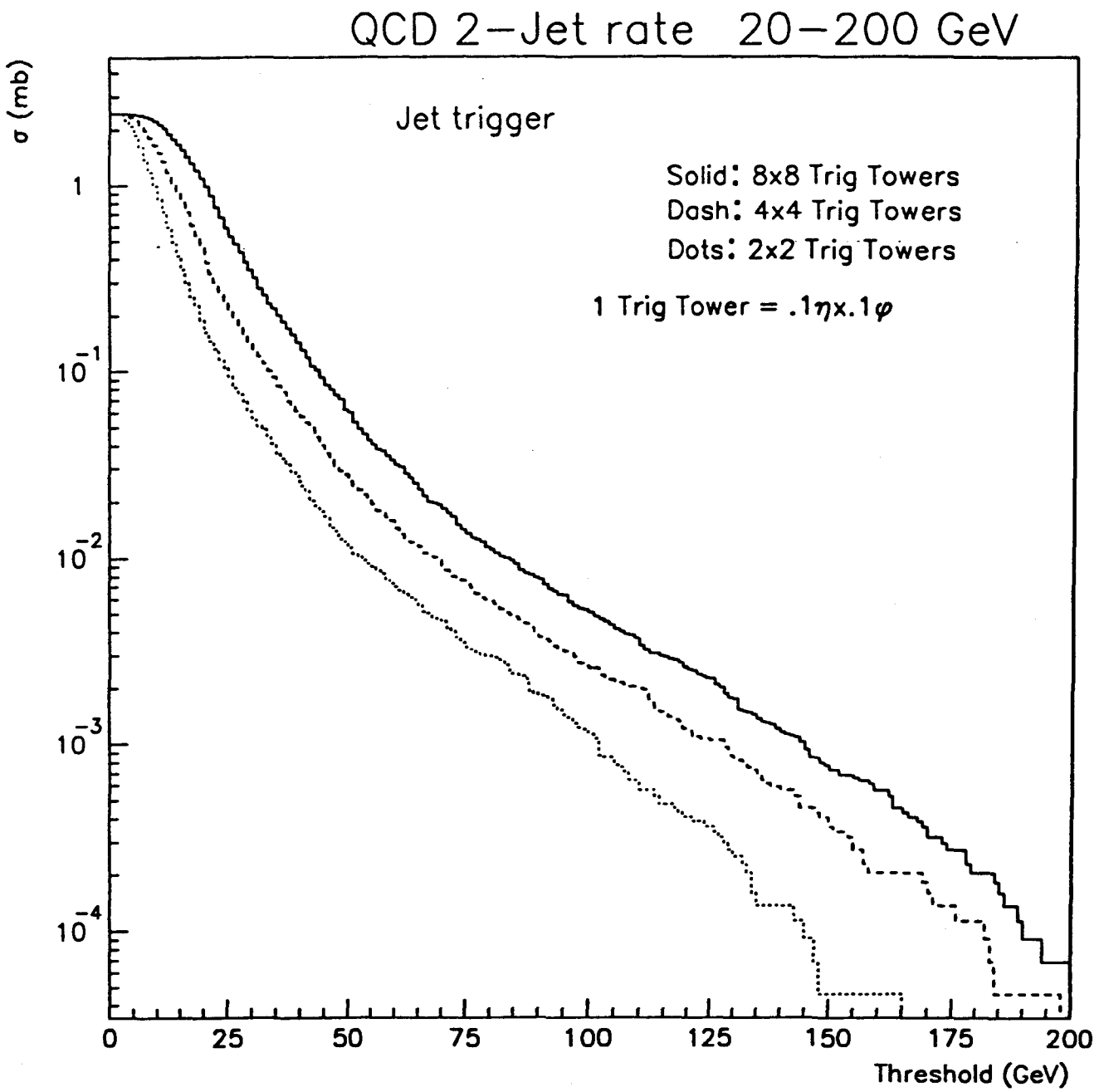


Figure 1: The level 1 inclusive jet trigger rate versus the $E_T$ threshold for various tower sizes.

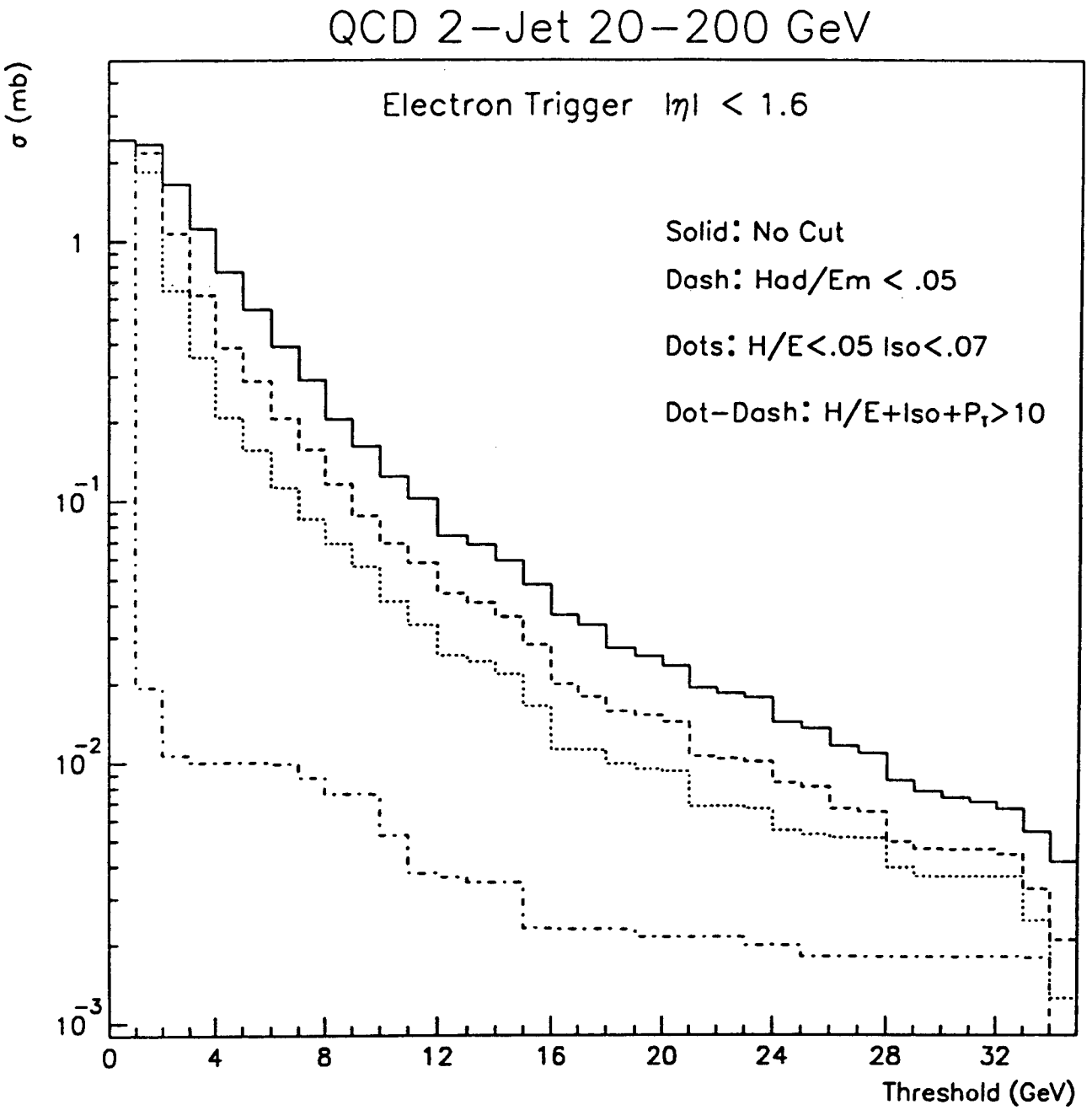


Figure 2: The level 1 inclusive electron trigger rate in the barrel calorimeter versus the $E_T$ threshold for no cut (solid), Had/Em cut (dashed), Had/Em and isolation (dot), and finally adding the requirement of a track match in $\phi$ with the tower (dot-dash).

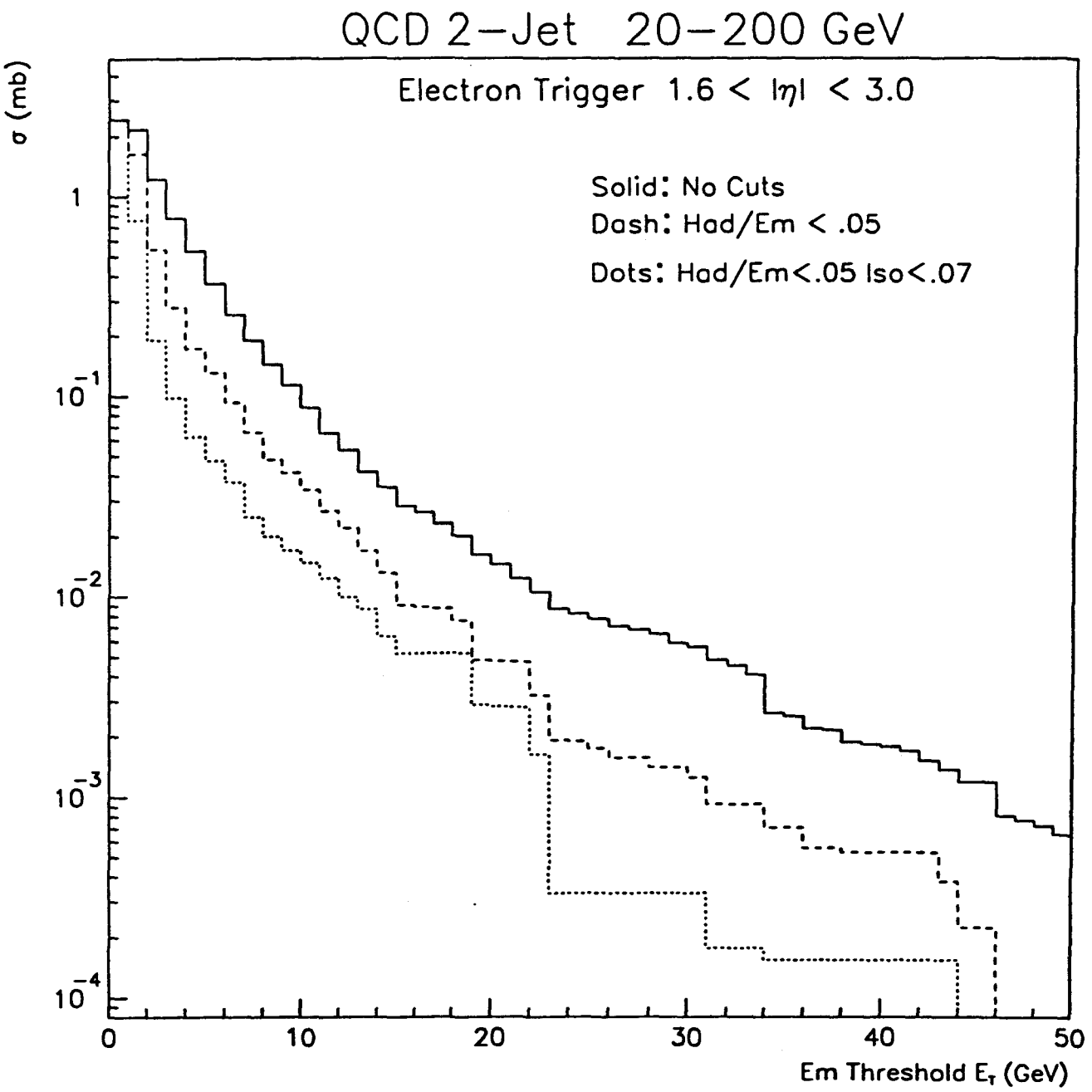


Figure 3: The level 1 inclusive electron trigger rate in the endcap calorimeter versus the $E_T$ threshold for no cut (solid), Had/Em cut (dashed), Had/Em and isolation (dot).

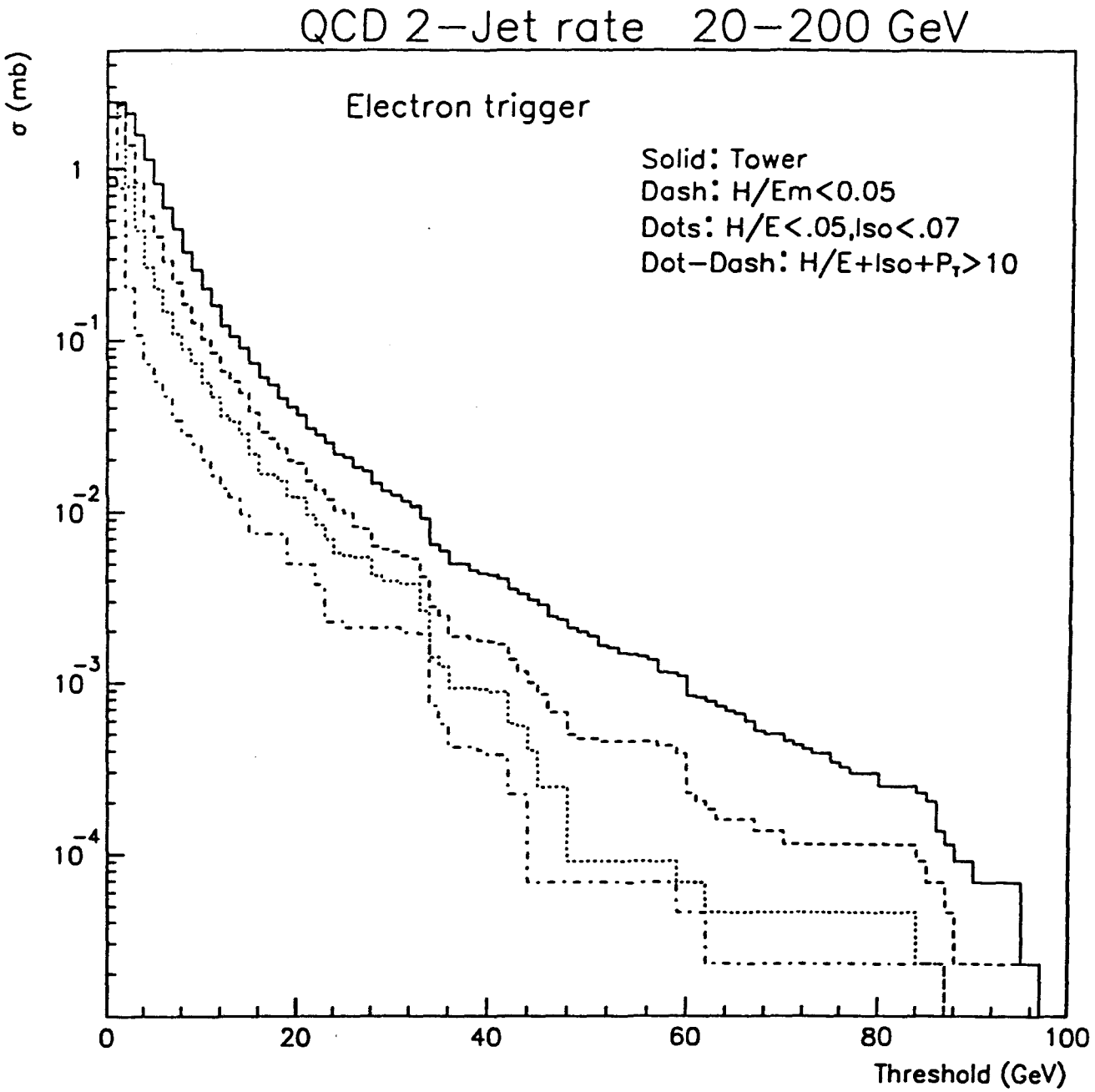


Figure 4: The level 1 inclusive electron trigger rate in the calorimeter ($\eta \leq 3.0$) versus the $E_T$ threshold for no cut (solid), Had/Em cut (dashed), Had/Em and isolation (dot), and finally adding the requirement of a central ($\eta \leq 1.6$) track match in $\phi$ with the tower (dot-dash).

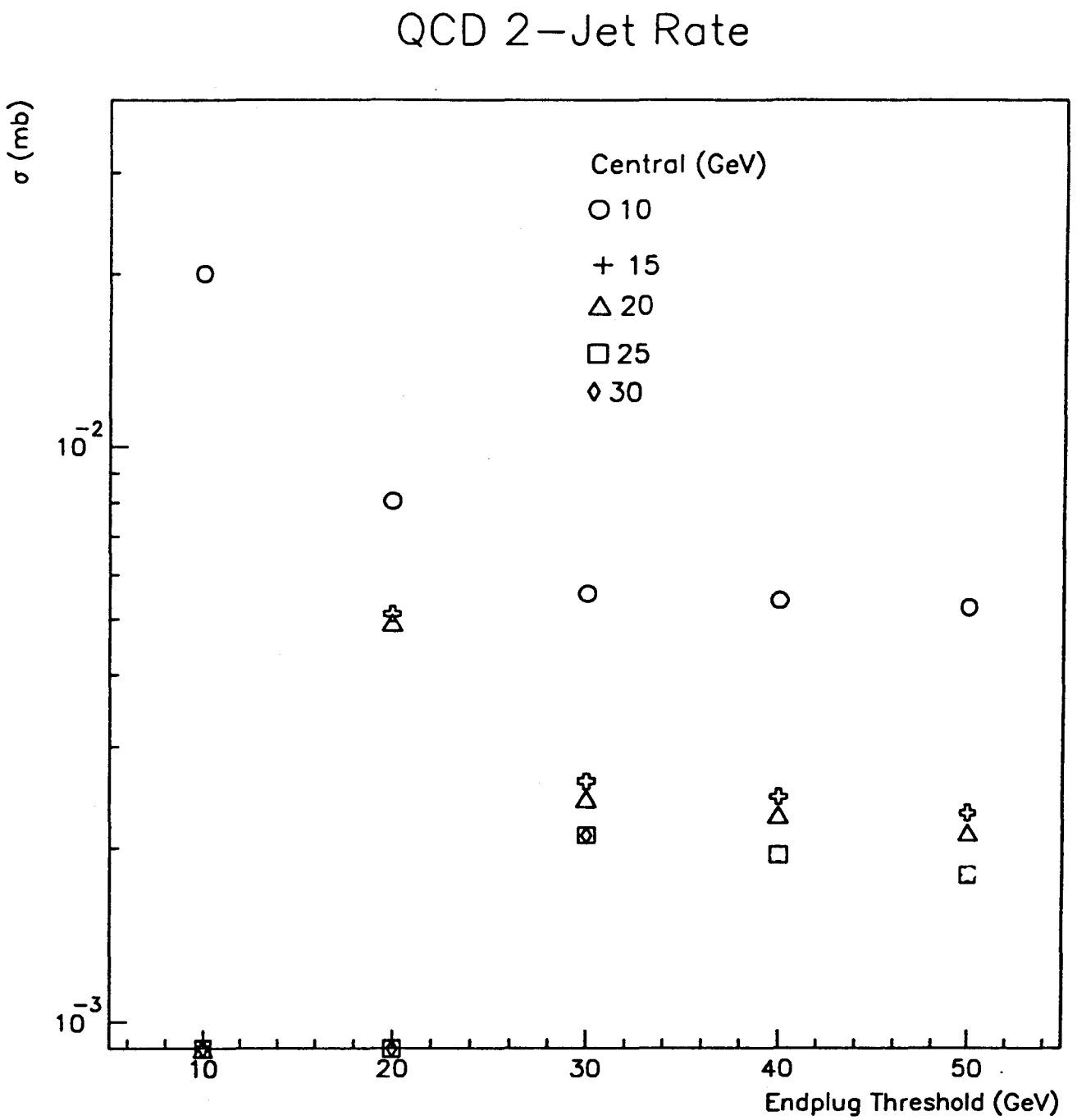


Figure 5: The level 1 inclusive electron trigger rate versus endplug $E_T$ threshold for various barrel $E_T$ thresholds. In all cases Had/EM < 0.05, Iso < 0.07, and central $p_T > 10.$.

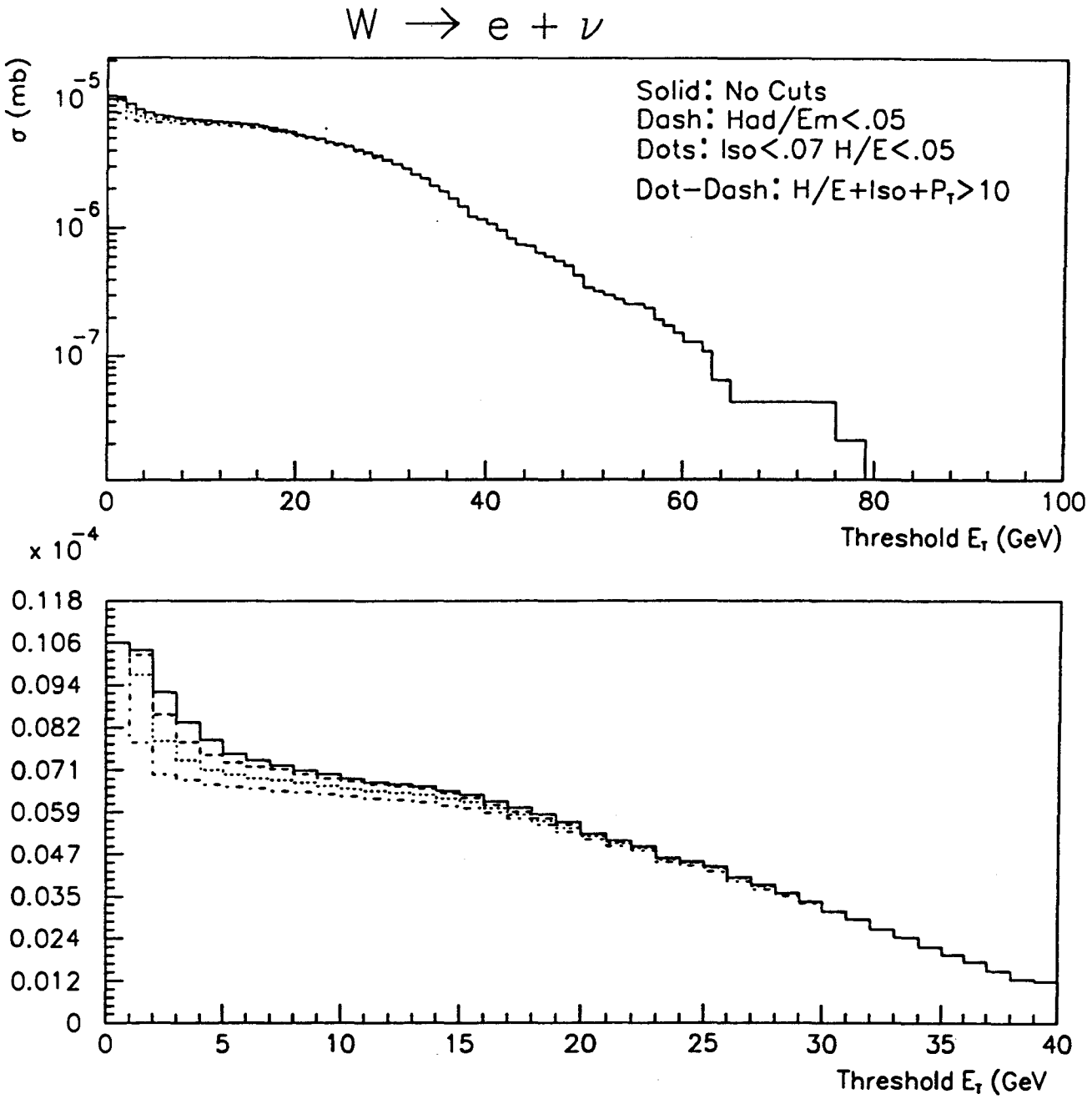


Figure 6: The W → e$\nu$ rate ($\eta \leq 3.0$) versus $E_T$ threshold for no cut (solid), Had/Em cut (dashed), Had/Em and isolation (dot), and finally adding the requirement of a central ($\eta \leq 1.6$) track match in $\phi$ with the tower (dot-dash).

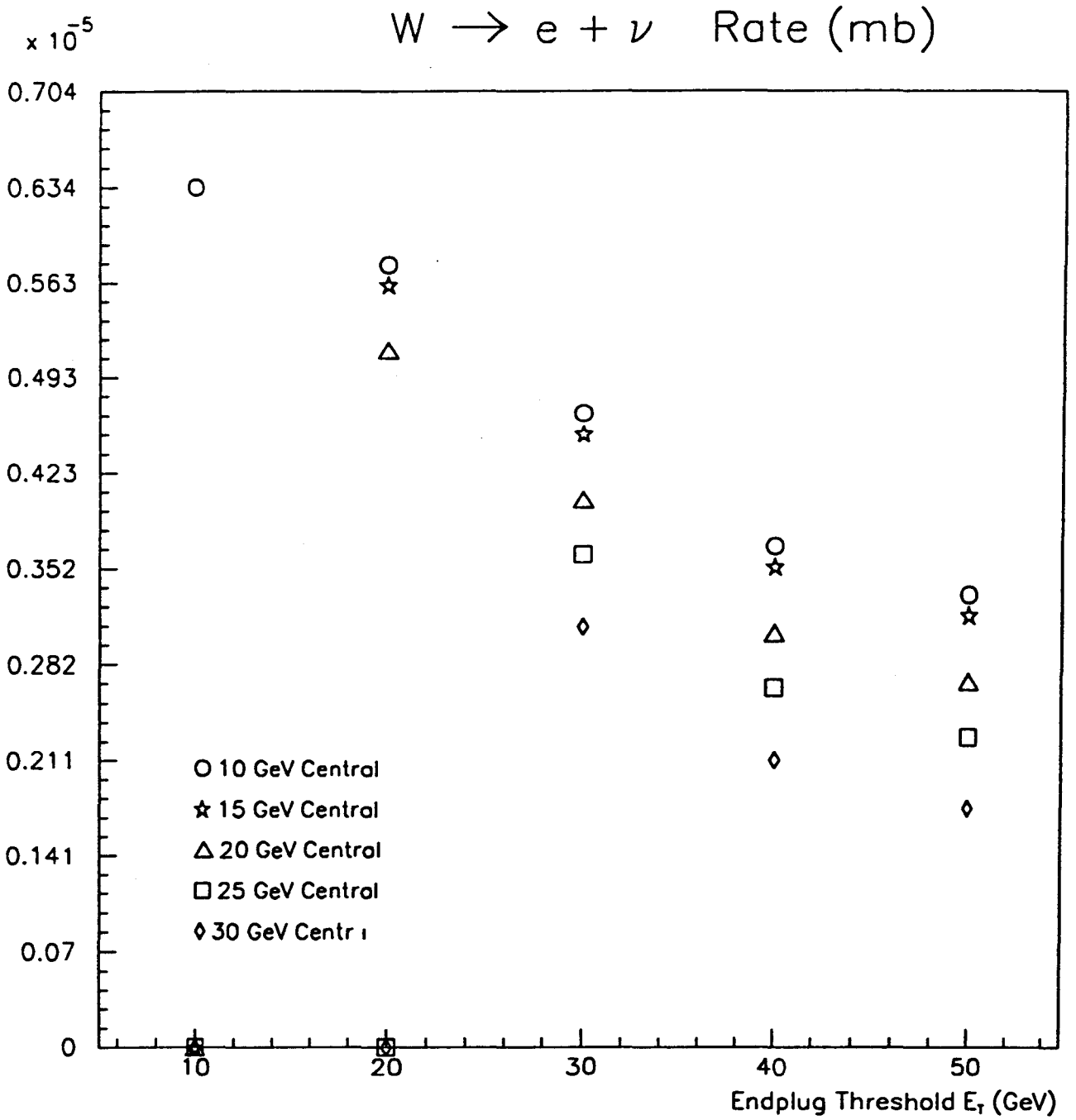


Figure 7: The W $\rightarrow e\nu$ trigger rate ($\eta \leq 3.0$) versus endplug $E_T$ threshold for various barrel $E_T$ thresholds. In all cases Had/EM < 0.05, Iso < 0.07, and central $p_T > 10$..

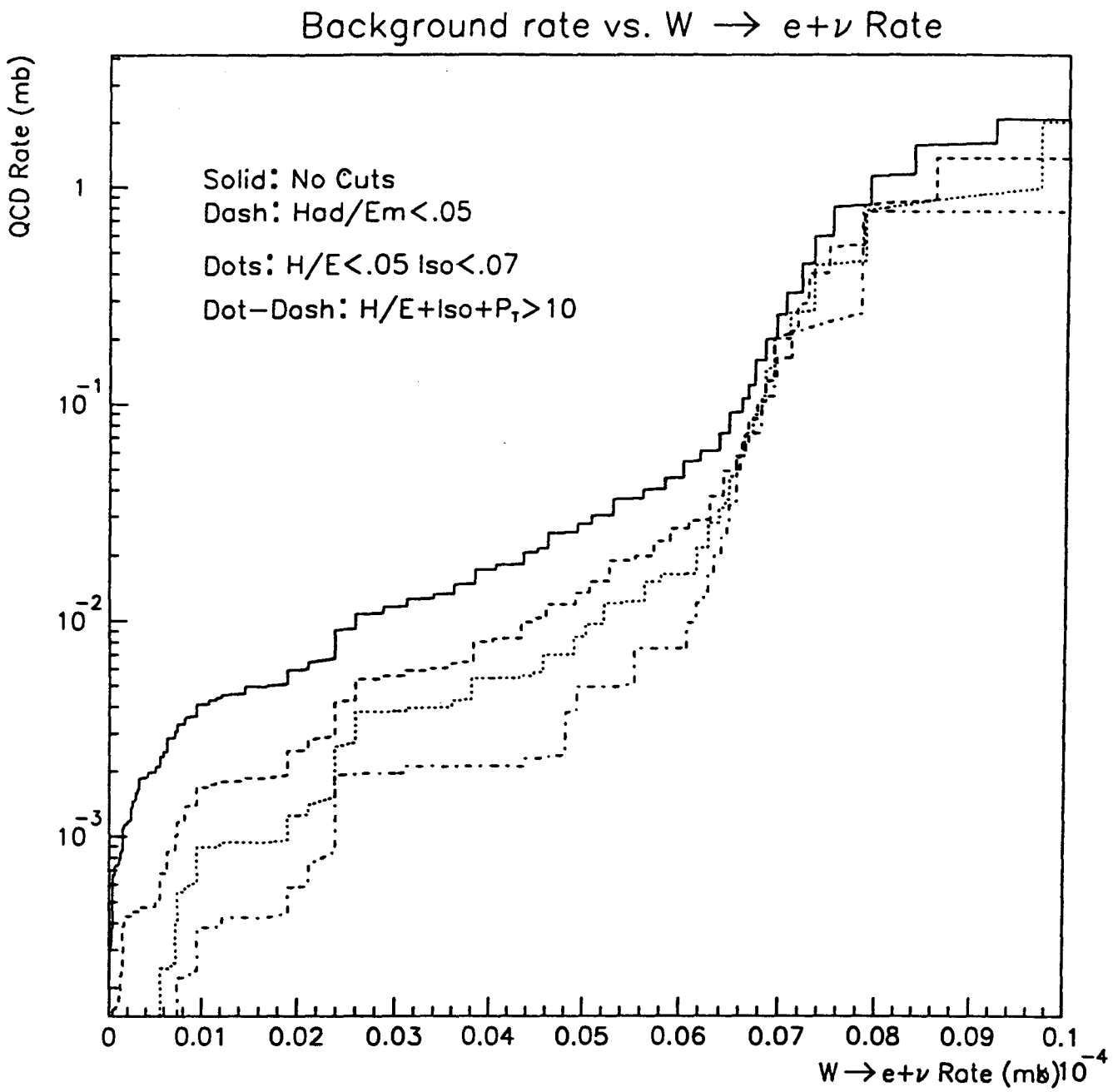


Figure 8: The QCD TWOJET background rate versus the W $\rightarrow$ e$\nu$ trigger rate ($\eta \leq 3.0$) for no cut (solid), Had/Em cut (dashed), Had/Em and isolation (dot), and finally adding the requirement of a central ($\eta \leq 1.6$) track match in $\phi$ with the tower (dot-dash).

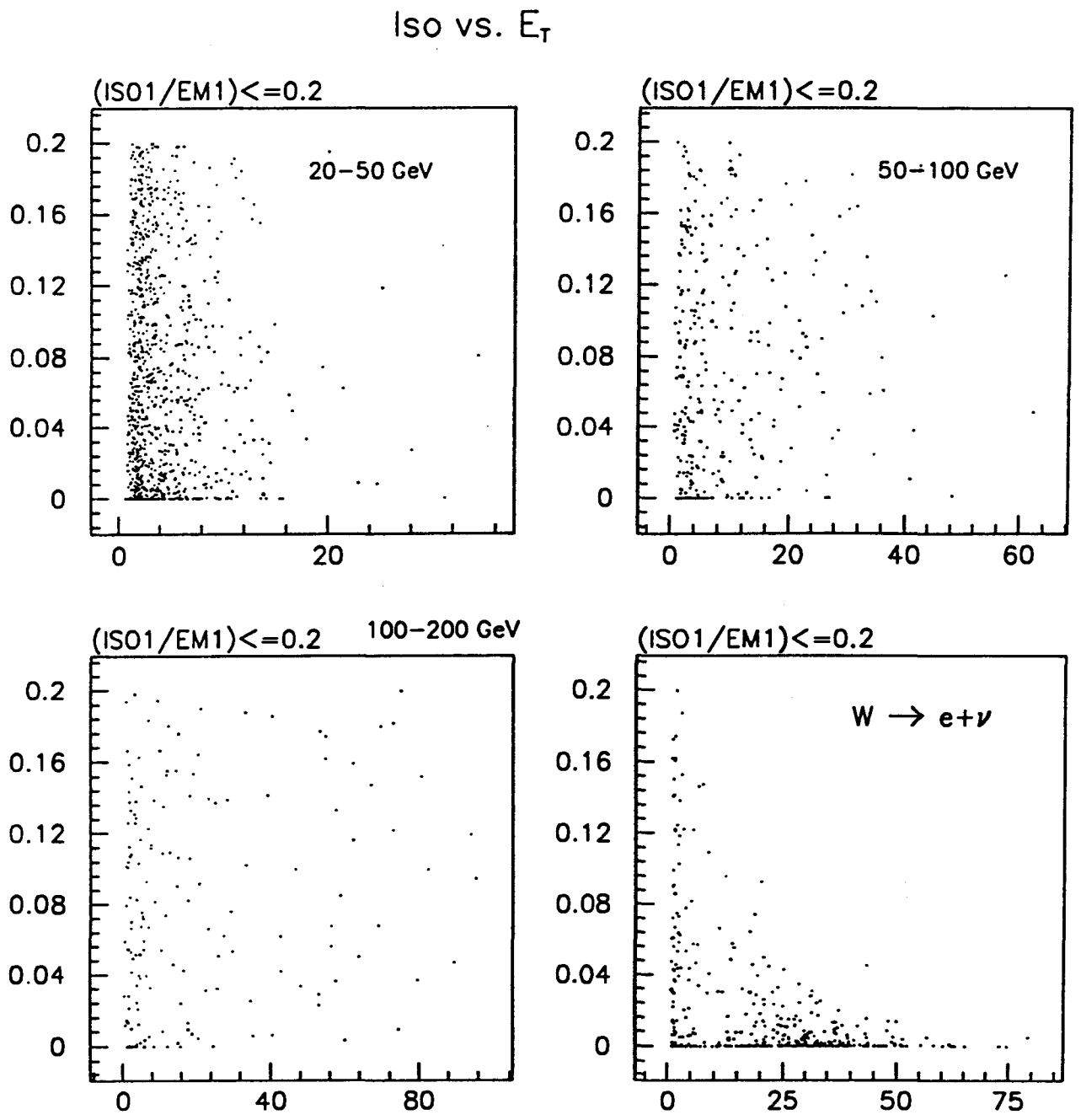


Figure 9: Isolation versus highest $E_T$ tower for the three QCD TWOJET samples and the $W \rightarrow e\nu$ sample.

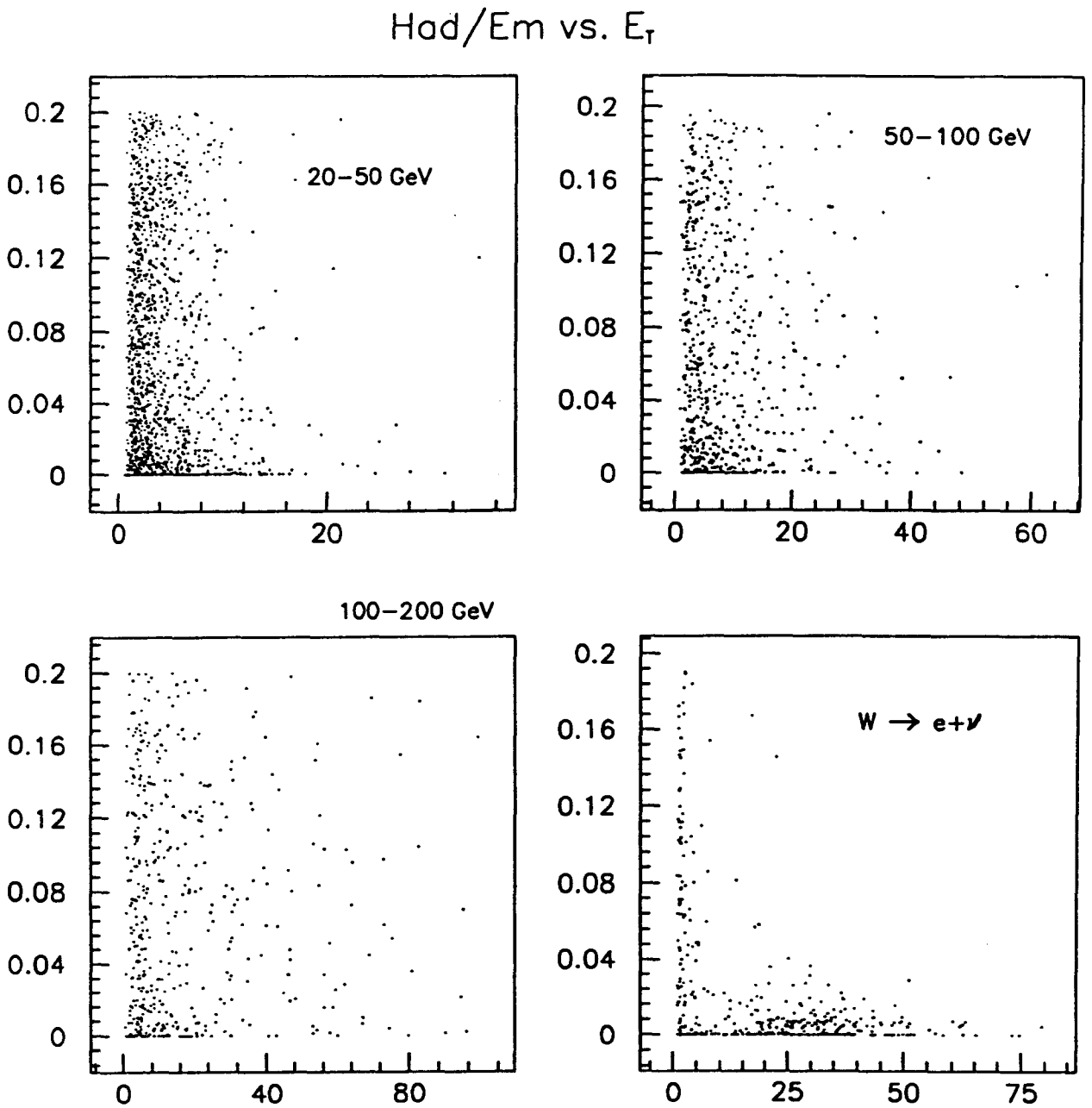


Figure 10: Had/EM versus highest $E_T$ tower for the three QCD TWOJET samples and the $W \rightarrow e\nu$ sample.